Journal of Exposure Science & Environmental Epidemiology (2020) 30:1013–1022
https://doi.org/10.1038/s41370-019-0146-1

ARTICLE

Estimating personal exposures from a multi-hazard sensor network

Christopher Zuidema[1,2] · Larissa V. Stebounova[3] · Sinan Sousan[3,4,5] · Alyson Gray[3] · Oliver Stroh[6] · Geb Thomas[6] · Thomas Peters[3] · Kirsten Koehler[1]

Received: 12 December 2018 / Revised: 11 April 2019 / Accepted: 10 May 2019 / Published online: 4 June 2019

Abstract

Occupational exposure assessment is almost exclusively accomplished with personal sampling. However, personal sampling can be burdensome and suffers from low sample sizes, resulting in inadequately characterized workplace exposures. Sensor networks offer the opportunity to measure occupational hazards with a high degree of spatiotemporal resolution. Here, we demonstrate an approach to estimate personal exposure to respirable particulate matter (PM), carbon monoxide (CO), ozone (O_3), and noise using hazard data from a sensor network. We simulated stationary and mobile employees that work at the study site, a heavy-vehicle manufacturing facility. Network-derived exposure estimates compared favorably to measurements taken with a suite of personal direct-reading instruments (DRIs) deployed to mimic personal sampling but varied by hazard and type of employee. The root mean square error (RMSE) between network-derived exposure estimates and personal DRI measurements for mobile employees was 0.15 mg/m^3, 1 ppm, 82 ppb, and 3 dBA for PM, CO, O_3, and noise, respectively. Pearson correlation between network-derived exposure estimates and DRI measurements ranged from 0.39 (noise for mobile employees) to 0.75 (noise for stationary employees). Despite the error observed estimating personal exposure to occupational hazards it holds promise as an additional tool to be used with traditional personal sampling due to the ability to frequently and easily collect exposure information on many employees.

Keywords low-cost sensors · sensor networks · personal sampling · area sampling · exposure assessment

Introduction

Occupational environments, especially heavy industry, often have complex hazardous exposures resulting from manufacturing processes including cutting metal stock, welding, grinding, machining, and abrasive blasting. Exposures resulting from these processes include particulate matter (PM); gases such carbon monoxide (CO), oxides of nitrogen (NO_x), and ozone (O_3); metals including lead, nickel, zinc, manganese, iron oxides, copper, cadmium and chromium; physical hazards such as noise, heat, electrical and vibration; and radiological including visible and ultra-violet frequencies of light [1]. To assess compliance with occupational exposure limits to workplace hazards, employers have historically performed exposure monitoring, typically by personal sampling on individuals suspected to have high exposure [2]. However, personal sampling can have drawbacks such as high expense and burden to employees and generally suffers from a low number of samples taken [3]. In most cases, fewer than six samples at an industrial facility are used to judge if employees may be over-exposed or workplaces are in

Supplementary information The online version of this article (https://doi.org/10.1038/s41370-019-0146-1) contains supplementary material, which is available to authorized users.

✉ Kirsten Koehler
kirsten.koehler@jhu.edu

1 Department of Environmental Health and Engineering, Johns Hopkins Bloomberg School of Public Health, Baltimore, MD, USA

2 Department of Occupational and Environmental Health Sciences, University of Washington School of Public Health, Seattle, USA

3 Department of Occupational and Environmental Health, University of Iowa, Iowa City, IA, USA

4 Department of Public Health, East Carolina University, Greenville, NC, USA

5 North Carolina Agromedicine Institute, Greenville, NC, USA

6 Department of Industrial and Systems Engineering, University of Iowa, Iowa City, IA, USA

compliance with regulatory permissible exposure limits [4], and many rely on just one measurement [5]. This situation results in inadequately characterized workplace exposures and occupational risks that may be higher than compliance testing indicates [3].

In light of this problem, the National Institute for Occupational Safety and Health (NIOSH) has called for "comprehensive exposure assessment," where risks from all hazards for all days and all workers are considered [6]. Furthermore, cost-efficient occupational exposure assessment, where both economics and statistical efficiency (e.g. number of subjects, sample size and measurement error) are considered, is also needed [7]. Low-cost sensors could potentially fill this need and have recently attracted the attention of environmental health scientists seeking to measure air pollution with a high degree of temporal and spatial resolution, for example compared to commonly used daily averages [8–12]. Advances in open software toolkits and microprocessor platforms have facilitated the development of customized wireless sensor networks, and there is a growing number of examples in the literature [13–22]. Data from sensor networks may be used to create hazard maps [23–31], which visually communicate risk [32], identify hazard sources [24, 27], characterize the distribution of hazards in a facility or the environment [26, 27, 31], and inform hazard control strategies [24].

We have previously developed a multi-hazard sensor network constructed with low-cost sensors for PM, CO, oxidizing gases ($O_3 + NO_2$) and noise [33]. An industrial hygienist identified hazards at the study site, a heavy-vehicle manufacturing facility, and those of greatest occupational health importance were chosen for inclusion our sensor network. PM has well-characterized associations with cardiopulmonary and respiratory diseases, lung cancer, inflammation, oxidative stress, pulmonary infection, and lung function [34–37]. The health effects of occupationally relevant CO concentrations include headache, dizziness, weakness, nausea and confusion [38]. The inhalation of O_3 causes inflammation, reduced lung function, DNA damage and increased symptoms and development of asthma [39–42]. Occupational noise exposure induces hearing impairment, hypertension and annoyance [43]. Additionally, there is limited evidence that noise in the workplace is associated with biochemical and immune effects, and impacts absentee rate and performance [43].

In previous work, we have described the long-term deployment of our multi-hazard sensor network capable of mapping PM, CO, oxidizing gases and noise at the study site with a high degree of spatial and temporal resolution [44]. In the current study we demonstrate that hazard mapping data from a multi-hazard sensor network, when combined with an individual's location information, can be used to quantitatively estimate personal exposure to multiple occupational hazards simultaneously. We compare the network-derived exposure estimates to personal measurements collected from high-quality, personal direct-reading instruments that are commonly used in industrial hygiene practice.

Materials and methods

Sensor network

We designed and constructed multi-hazard monitors, the sensors for which are summarized in Table S1. Each monitor, or "node" of the sensor network was equipped with sensors to measure PM (GP2Y1010AU0F, Sharp Electronics, Osaka, Japan); oxidizing gases (OX-B431, Alphasense Ltd., Essex UK; responsive to both O_3 and NO_2); CO (CO-B4, Alphasense Ltd., Essex UK); sound pressure level (SPL); [45] and temperature and relative humidity (AM2302, Adafruit, New York, NY) [33]. The 40-node network was installed for approximately eight months within 74,900 m^2 of a + 185,800 m^2 manufacturing facility that produces heavy vehicles for construction and forestry. The nodes of the network were deployed in a spatially optimized pattern to capture maximum spatial variability [46], and measurements from each monitor were transmitted wirelessly to a central database approximately every 5 min, permitting the hazard variability to be characterized with a high degree of spatial and temporal resolution.

We applied calibration curves developed in the laboratory for the CO and oxidizing gas sensors from a sample of three sensors of each type [47]. These calibration curves were then applied to all sensors of that type in the monitor network for the duration of the sensor network deployment. The noise sensor used in the network was custom-made for this project [45]. Briefly, each of the sensors were calibrated over a range of 65 to 95 dB with an acceptance criterion of ±2 dB with respect to a high quality direct-reading instrument (XL2, NTi Audio AG, Liechtenstein).

For PM, a field-derived slope was applied to each monitor based on values obtained at a calibration site with a direct-reading instrument (pDR-1000, Thermo Scientific, Franklin, MA) [44]. Because neither the pDR-1000 nor the PM sensors are size selective, the average of five respirable fraction filter samples taken over the course of the sensor network deployment were used to gravimetrically correct the photometric PM concentrations (both the pDR-1000 and PM sensors). We took an additional step to correct PM sensor drift over the eight-month deployment by deriving sensor-specific weekly field calibration intercepts for each sensor. We did this by setting the average millivolt (mV) value of each sensor between 0000 and 0200 hours every

Sunday night when PM concentrations were lowest, equal to the sensor LOD (0.026 mg/m^3) [44]. The PM sensors in our network are affected by relative humidity (RH), but the impact on performance up to 67% RH is small [48], and since RH in this study was typically well below that, we made no RH correction (%RH mean ± standard deviation: 26 ± 10%). The effect of temperature on the PM sensor was negligible [48].

For each of the sensor types in the network, we imputed all sensor measurements that were below the sensor limit of detection (LOD) with a value of the LOD divided by the square root of two (LODs: PM [49] = 0.026 mg/m^3; CO = 10 ppb; OX-B431 [50] = 4 ppb; noise [45] = 65 dBA). We have previously reported on the spatial and temporal variability of hazards, sensor precision, and measurement accuracy in the facility [44].

Worker simulation and personal DRIs

On five occasions in August 2017, December 2017, and March 2018 we simulated two types of workers. The first type of worker was one that was highly mobile and traveled throughout the facility at a walking or slow biking/driving pace, such as supervisors, mechanics, employees that move small parts between workstations, and maintenance workers. For the first type of simulated worker, personal DRIs were worn by study staff, as a worker would for traditional personal sampling. Hereafter we refer to this simulated employee type as the "mobile" routine. For the mobile sampling routines, study staff kept a detailed log of their position as they moved throughout the facility according to an established coordinate system, marked by regularly spaced structural I-beams. The second type of worker was one that remained in a relatively small geographic space (within an area ≤12 × 18 m) to perform their work duties, such as a welder or machine operator. For this type of simulated worker, personal DRIs were deployed at an employee workstation for the duration of the simulated work shift and were not moved. Hereafter we refer to this simulated employee type as the "stationary" routine. We simulated a total of 22 work shifts (5 mobile and 17 stationary) during times of typical production (weekdays, 0600–1600 hours). The personal DRIs were as follows: respirable PM, personal DataRAM 1500 configured for respirable dust sampling ('pDR-1500,' Thermo Scientific, Franklin, MA); CO, EasyLog CO-300 (Lascar Electronics Ltd., Erie, PA); O_3, Personal Ozone Monitor ('POM,' 2BTechnologies, Boulder, CO); and noise, Spark 703 + (Larson-Davis Inc., Depew, NY). The personal DRIs used in this study for each hazard are shown in Table S1 alongside the low-cost sensors in the sensor network. These DRIs were chosen for personal measurements because they were representative of typical instruments commonly used for occupational exposure assessment by industrial hygienists and health and safety professionals.

Network-derived exposure estimates

schematic representation of our method for computing sensor network-derived exposure estimates is depicted in Fig. 1, where two pieces of information are integrated: (1) the location of the simulated worker and (2) the hazard intensity at the position of interest. The blue line indicates the route traveled by a simulated employee and the blue "X"

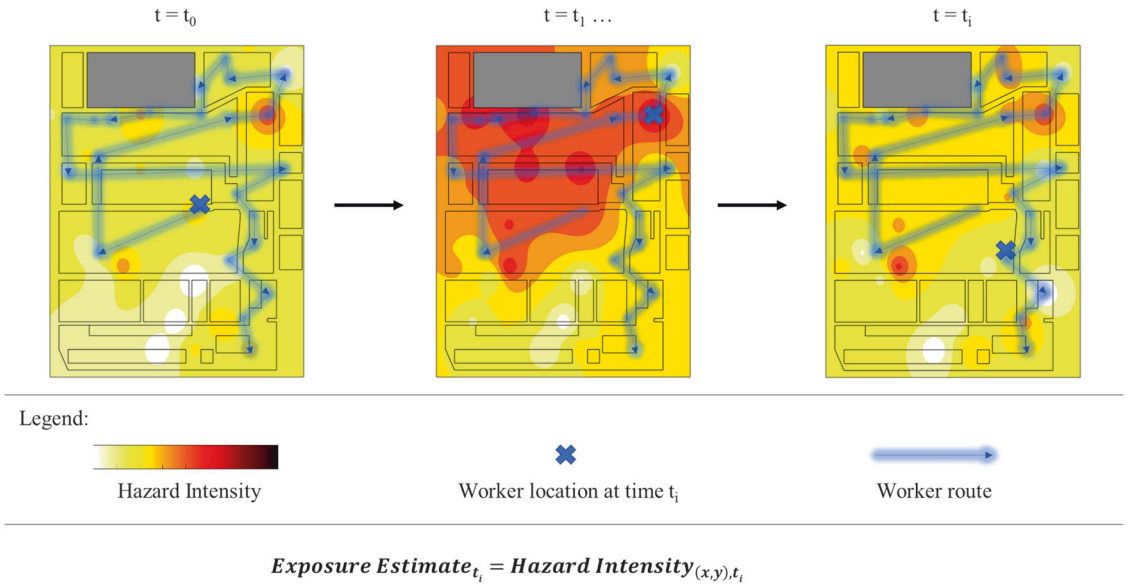

$$Exposure\ Estimate_{t_i} = Hazard\ Intensity_{(x,y),t_i}$$

Fig. 1 Schematic of technique to estimate personal exposure from the sensor network. Exposure estimates are derived by taking the hazard intensity at location (x, y) for time t_i, over the time period of interest

indicates the location of the employee at a given time (t_0, t_1… t_i). Hazard intensity is represented by hazard maps, and for each time of interest, t_i, we estimated the hazard intensity, at the location of interest, (x,y). We used an inverse distance weighting (IDW) scheme to interpolate hazard intensity at unmeasured locations, which are displayed as a hazard maps for each 5-min period. Interpolating hazard intensity with IDW is physically plausible and computationally practical. We chose inverse distance squared weighting because it is supported by previous studies [32]. Location and time information for the mobile sampling routine was recorded at every movement of study staff as they traveled throughout the facility, generally following a pattern of walking for 1–2 min (covering approximately 24–41 m), remaining stationary for 5–15 min and walking again to the next location. Location for the stationary routine was taken as the coordinate where the suite of personal DRIs was deployed and did not change for the duration of the sampling period. Because the sensor network recorded hazard measurements every 5 min, we constructed hazard estimates at 5-min intervals also (e.g. $t_0 = 0700$, $t_1 = 0705$. $t_i = 0700 + 0005 \cdot i$). Data analysis was performed with MATLAB R2017a (Natick, MA), with exception of descriptive noise calculations which were carried out in R 3.5.2 (Vienna, Austria) with the 'seewave' package [51].

Data analysis & comparing network-derived estimates and personal DRI measurements

For each routine we paired 5-min network-derived exposure estimates with 5-min personal DRI measurements and performed all analysis on paired 5-min data. For each simulated work shift we plotted a timeseries of the network-derived exposure estimates with the personal DRI measurements timeseries to qualitatively assess their overall agreement and correlation. We created "Bland–Altman" plots [52] displaying the difference versus the mean of network-derived exposure estimates and measurements taken with personal DRIs to compare their agreement. These plots show the mean difference between the network-derived exposure estimates and the personal DRI measurements and the limits of agreement (the mean difference ±2σ). For differences that are normally distributed, 95% of the data will fall within the limits of agreement.

We pooled the 5-min pairs of network-derived exposure estimates and personal DRI measurements by simulated employee type (mobile or stationary) and by the month collected (August 2017, December 2017, March 2018, and August, December and March combined) for the following summary statistics: number of paired network-derived exposure estimates and personal DRI measurements, root mean squared error (RMSE), Pearson correlation, and relative agreement computations. We performed a regression-based comparison between network-derived exposure estimates and personal DRI measurements and calculated the RMSE and Pearson correlation coefficient. We tabulated a relative measure of agreement between network-derived estimates and personal DRI measurements by calculating the fraction of network-derived exposure estimates that were within (±) 10, 25, 50 and 100% of the personal DRI measurements.

Results

Examples of timeseries for the August 2017 sampling period comparing network-derived mobile exposure estimates to personal DRI measurements are shown in Fig. 2. The results of all personal DRI measurements and

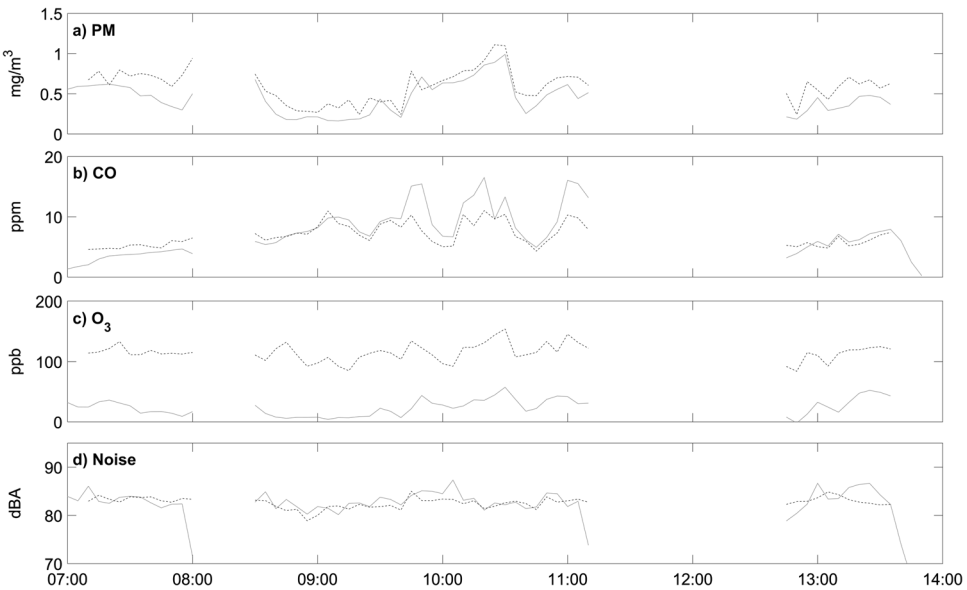

Fig. 2 Examples of timeseries comparing network-derived exposure estimates (dashed line) with personal DRI measurements (solid line) for a simulated mobile employee for **a** PM, **b** CO, **c** O_3, and **d** noise over the course of one work shift

network-derived exposure estimates are summarized in Table 1 (mobile routine) and Table S2 (stationary routine). We collected data for one mobile and three stationary routines on 1 day in August 2017, two mobile and six stationary routines over 2 days in December 2017, and two mobile eight stationary routines over 2 days in March 2018. The number of 5-min pairs of network-derived exposure estimates and personal DRI measurements, N, ranged between 55 (all hazards, August 2017) and 169 (CO, March 2018). The number of 5-min pairs differed between hazards and time periods due to instrument allocation, run times and equipment failures. For example, in December 2017 for two mobile routines of ~6 h each we collected a total of 156 pairs of 5-min network-derived exposure estimates and personal DRI measurements for both CO and noise. In comparison, we collected 153 pairs for PM due to a difference in run-time and only 91 pairs for O_3, due to personal DRI failure.

The geometric mean (GM) and arithmetic means (AM) of PM, CO, O_3 and noise measured by the personal DRIs varied between each of the sampling periods (August 2017 vs. December 2017 vs. March 2018), are shown in Table 1 (mobile routine) and Table S2 (stationary routine). Mean hazard intensities generally reflected manufacturing activity in the facility, specifically, production in the facility during the December 2017 period was low due to the upcoming holiday shutdown, and comparatively higher for the March 2018 period. For example, the lowest PM concentrations were observed for both mobile and stationary personal DRI measurements in December 2017 (GM PM concentrations: mobile = 0.30 mg/m^3; stationary = 0.20 mg/m^3) and were highest in March 2018 (GM PM concentrations: mobile = 0.48 mg/m^3; stationary = 0.58 mg/m^3). Other hazards displayed similar patterns but differences between sampling periods were not as notable as those observed for PM. None of the 5-min personal DRI measurements were below the instrument's LOD for PM, and noise. For CO 2%, and for O_3, 0.3% of DRI measurements were below the instrument's LOD.

Comparisons of mobile routine personal DRI measurements and network-derived exposure estimates are shown in Table 1. In the mobile routine for the combined time period

Table 1 Comparison of personal DRI measurements and network-derived exposure estimates (pairs of 5-min averages) for the mobile routine

Hazard	Time Period	# Simulated Work Shifts, K	# 5-min Pairs, N	DRI GM (GSD)	DRI AM (ASD)	RMSE	Pearson Correlation	Fraction within Percent of DRI[a]			
								10	25	50	100
PM						units: mg/m^3					
	Aug-2017	1	55	0.40 (1.62)	0.44 (0.20)	0.11	0.84	0.11	0.36	0.62	0.87
	Dec-2017	2	153	0.28 (1.47)	0.30 (0.11)	0.09	0.60	0.18	0.41	0.7	0.92
	Mar-2018	2	162	0.48 (1.58)	0.52 (0.21)	0.16	0.39	0.15	0.3	0.7	0.98
	Combined	**5**	**370**	**0.37 (1.65)**	**0.42 (0.20)**	**0.15**	**0.47**	**0.16**	**0.36**	**0.69**	**0.94**
CO						units: ppm					
	Aug-2017	1	55	4 (7)	7 (4)	1	0.86	0.25	0.64	0.91	0.98
	Dec-2017	2	156	5 (1)	5 (2)	1	0.59	0.25	0.63	0.9	1
	Mar-2018	2	169	3 (6)	4 (3)	1	0.41	0.22	0.53	0.72	0.84
	Combined	**5**	**380**	**3 (4)**	**5 (3)**	**1**	**0.66**	**0.24**	**0.58**	**0.82**	**0.93**
O_3						units: ppb					
	Aug-2017	1	55	19 (2)	24 (14)	11	0.63	0.02	0.02	0.02	0.02
	Dec-2017	1	91	29 (1)	30 (9)	24	0.05	0	0	0	0.03
	Mar-2018	2	168	111 (2)	130 (71)	31	0.54	0.12	0.37	0.7	0.84
	Combined	**4**	**314**	**54 (3)**	**82 (73)**	**27**	**0.54**	**0.07**	**0.2**	**0.38**	**0.46**
Noise						units: dBA					
	Aug-2017	1	55	83 (3)[b]		1	0.23	0.96	1	1	1
	Dec-2017	2	156	83 (3)[b]		2	0.43	0.96	1	1	1
	Mar-2018	0	0	–		–	–	–	–	–	–
	Combined	**3**	**211**	**83 (3)[b]**		**3**	**0.39**	**0.96**	**1**	**1**	**1**

Equipment failure resulted in no personal noise measurements in March 2018

GM geometric mean, *GSD* geometric standard deviation, *AM* arithmetic mean, *ASD* arithmetic standard deviation, *RMSE* root mean square error

[a]Fraction of network-derived exposure estimates that were within (±) 10, 25, 50 and 100% of the personal DRI measurements for each hazard

[b]Noise calculations were performed on data transformed to the linear scale then transformed back to the dBA scale, and are not technically GMs and GSDs

the RMSEs between network-derived estimates and DRI measurements were 0.15 mg/m^3, 1 ppm, 27 ppb, and 3 dBA for PM, CO, O_3 and noise, respectively. For PM, CO, and noise there was little variation in the RMSE between August 2017, December 2017 and March 2018. We observed greater variability in the RMSE for O_3, which increased over time, from 11 ppb in August 2017 to 31 ppb in March 2018—likely related to the generally higher O_3 concentrations observed in March 2018 which were associated with larger differences between network-derived exposure estimates and personal DRI measurements. The correlation observed between the network-derived exposure estimates and their respective personal DRIs for each hazard also varied for the mobile routine. The combined Pearson correlation was highest for CO ($r = 0.66$), whereas the lowest was for noise ($r = 0.39$). In the mobile routine, as with the stationary routine, the fraction of network-derived exposure estimates within a given percentage of the personal DRI measurements was highest for noise. For example, 0.96 of the combined noise estimates were within 10% of the personal DRI, compared to 0.24 for CO, 0.16 for PM and 0.07 for O_3. Unfortunately, due to equipment failure in the March 2018 sampling period, no mobile noise personal DRI measurements were collected.

The Bland–Altman plots between network-derived exposure estimates and personal DRI measurements for the mobile routine are displayed in Fig. 3. For PM, CO, O_3, and noise the mean difference (limits of agreement) between the network-derived exposure estimates and the personal DRI measurements was equal to 0.00 (−0.39, 0.39) mg/m^3, 0 (−4, 4) ppm, 36 (−86, 158) ppb, and −3 (−9, 4) dBA, respectively. Differences between network-derived exposure estimates and personal DRI measurements were centered and evenly distributed near zero for PM and CO. For O_3, at higher concentrations network-derived exposure estimates were increasingly negatively biased compared to personal DRI measurements. For noise, network-derived exposure estimates were generally lower than personal DRI measurements across the range observed.

Results for the stationary routine are presented in the Supporting Information (Table S2 and Figure S1). Generally, we observed similarity between the stationary and mobile routines with respect to the fraction of network-derived exposure estimates that fell within 10, 25, 50, and 100% of their corresponding personal DRI measurements. Of all hazards, the combined network-derived exposure estimates for noise had the largest fraction of estimates within the smallest percentage of the personal DRI measurements for both the mobile and stationary routines, where 0.99–1.00 of network-derived exposure estimates were within 10% of personal DRI measurements.

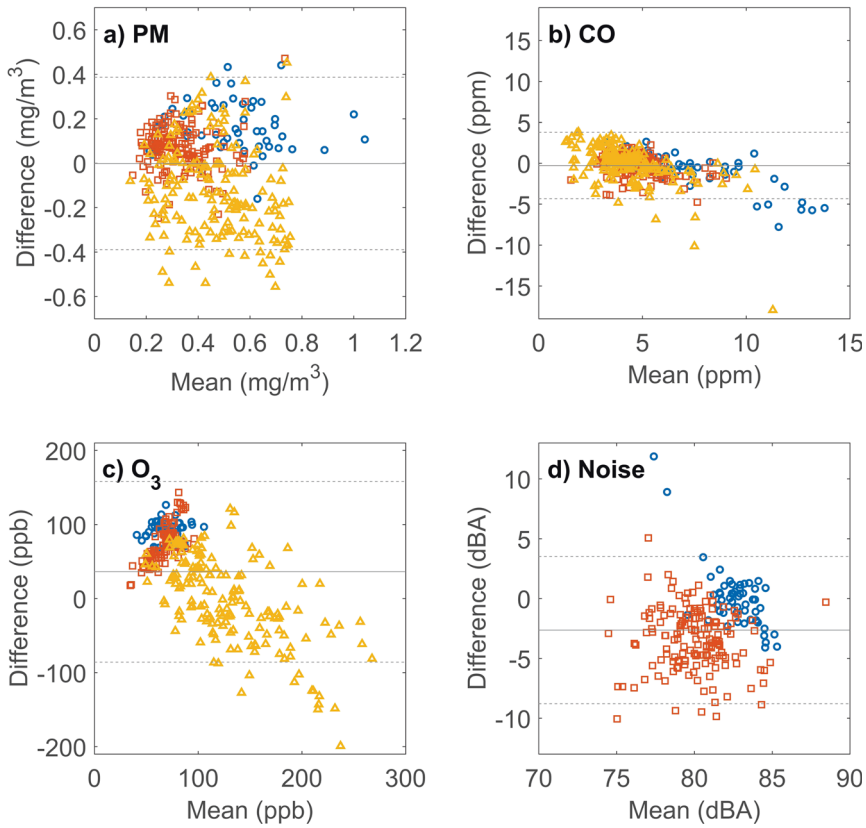

Fig. 3 Bland–Altman plots of the difference between network-derived exposure measurements and personal DRI measurements versus their mean for **a** PM, **b** CO, **c** O_3, and **d** noise. The solid line indicates the mean difference and the dashed lines are the bounds of agreement. Circles are data from August 2017, squares are data from December 2017, and triangles are data from March 2018

In contrast, the hazard with the lowest fraction of network-derived exposure estimates within 100% of personal DRI measurements was O_3 for both routines, with only 0.45 for the combined stationary routine and 0.46 for the combined mobile routine.

The Pearson correlation between network-derived exposure estimates and personal DRI measurements varied by hazard, mobile versus stationary routine, and time period. Pearson correlation varied by hazard in the combined time periods of the mobile routines, it was highest for CO ($r = 0.66$) and lowest for noise ($r = 0.39$). Variability in correlation by routine was observed with noise, which had the biggest difference between the stationary routine ($r = 0.75$) and the mobile routine (0.39). An example of variability in correlation by sampling period, was observed for the mobile O_3 routine—in December 2017, the Pearson correlation coefficient was equal to 0.05, compared to August 2017 where it was equal to 0.63. These differences in correlation between hazards and stationary versus mobile routine could have been affected by the by the variability of the hazards during each study period and routine. For example, according to the personal DRIs, the combined GM (geometric standard deviation, GSD) for CO was equal to 3 (4) ppm for the mobile routine and 5 (3) ppm for the stationary routine; while noise had a combined mean (standard deviation) equal to 83 (3) dBA for the mobile routine and 81 (10) dBA for the stationary routine. The larger the range of the hazard intensity and the more evenly data are distributed across that range may result in higher correlation coefficients observed for some hazards and periods of time than others.

Discussion

The success of our approach estimating personal exposure highly depends on the accuracy of the underlying hazard measurements of the sensor network. We have previously reported on the accuracy of this sensor network's measurements by conducting experiments where each monitor was collocated with personal DRIs for one to 5 min [44]. In that study over a range of hazard intensities, we observed the magnitudes of the median percent bias between network monitors and DRIs were equal to 27%, 11%, 45% and 1%, for PM, CO, O_3 and noise respectively. In the same study, we observed higher levels of bias at lower hazard intensity—as high as 163 and 156% for PM and O_3, respectively.

While the sources of measurement error from low-cost sensors differ, they can often be attributed to issues of sensitivity and specificity, in part due to sensor drift or degradation over time or responsiveness to non-target species. The PM sensor in our network showed evidence of decreasing sensitivity over time due to sensor loading or fouling [33]. To reduce the effects of this drift on PM concentration estimates, we developed a procedure to correct the sensors weekly. In addition, the PM sensor in our network was not size selective, and there is evidence the sensors produce signals that vary with different PM composition or size distribution [53]. Future work to improve the accuracy of estimates from the sensor network include accounting for aerosol size and composition effects on the sensor response and additional in-field calibrations of all sensors. Sensor technology is continuously improving and emerging sensors may measure PM concentrations with lower bias in the future.

Our network was constructed with an oxidative gas sensor to estimate O_3 concentrations. In addition to O_3 the sensor also responds to NO_2 without discrimination [54, 55], complicating the estimation of O_3 in environments where NO_2 is also present. Future work may be able to incorporate the manufacturer's proposed method to pair an oxidizing gas sensor with and NO_2-specific sensor to improve the accuracy of O_3 measurements [54]. Another source of error in this study is a ceiling observed on the CO sensor as configured in our network at ~12 ppm CO [47], resulting from the optimization of the CO sensor signal for concentrations anticipated at the study site [33]. Because of this, the CO sensors are not sensitive to increasing CO concentrations above 12 ppm (totaling approximately 1% of all personal CO DRI measurements in this study). These errors in measurement translate to potential errors in estimating personal exposure. In contrast, the noise sensor, which was designed specifically for this sensor-network [45], did not show evidence of signal drift or degradation over time, and provided network-derived estimates agreeing most closely with the personal DRI measurements. However, despite the high agreement of the noise exposure estimates, in some sampling periods, the Pearson correlation coefficient was low ($r = 0.23$ for the August 2017 mobile routine), demonstrating that correlation between a sensor and personal DRI may not be the best measure of sensor performance.

Our approach of estimating exposure requires utilizing hazard measurements from a low-cost sensor network with high temporal and spatial resolution. Despite these challenging requirements, in this study we demonstrate it is feasible. The sensor network time resolution was 5 min; accordingly, we used a 5-min averaging time for the personal DRIs for comparison. Although a 5-min time resolution is high compared to shift-long time-weighted averages (TWAs), our approach was incapable of finer time resolution and may fail to accurately capture the peaks of brief high exposure events, especially for hazards that decay quickly, for example, impact or impulse noise. Another example is O_3, which is highly reactive and degrades quickly after it is produced. Limitations in temporal resolution especially affect the

estimates for employees that move through the facility at a rapid pace potentially covering large distances in the facility in 5 min, such as materials handlers or forklift operators. We were unable to simulate these types of rapidly moving employees in this study. To estimate hazard intensity at locations where nodes of the sensor network were not located, we interpolated hazard intensity using an IDW scheme. While this spatial interpolation undoubtedly introduced some degree of error, the nodes of our network were spatially dense, with the maximum distance to the nearest monitor equal to 40 m (135 ft), helping to avoid errors related to spatial interpolation. Still, the potential to mischaracterize the spatial variability of hazards, especially those that decrease rapidly from their sources remains. We examined the impact of the distance to the nearest sensor network node and did not observe a relationship with respect to the bias of network-derived exposure estimates and personal DRI measurements.

In this study for simulated mobile employees, location information was supplied by study staff keeping a location diary during the sampling period. Although this was necessary to demonstrate our approach for generating network-derived exposure estimates, it is not practical for employees or employers, and automated indoor positioning systems would reduce the burden for this type of exposure assessment. While previous exposure assessment studies have used Global Positioning Systems (GPS) successfully [56, 57], they unfortunately generally perform poorly indoors due to interference from building roofs and a lack of "line-of-sight" to the satellites [58]. Therefore, for indoor/occupational settings, technologies specifically capable of indoor localization are necessary. These indoor positioning systems include radio frequency identification (RFID), wireless local area networks (WLAN), indoor GPS, and ultra-wide band radio frequency [59–61], and have been investigated in construction, manufacturing, warehouses, agriculture and healthcare settings [60, 62–66]. Future work will focus on the use of indoor positioning systems such as these to provide location information for generating exposure estimates derived from a low-cost sensor network in an occupational setting.

Despite these challenges, this study had many novel features and strengths. This is the first example of using a sensor network to estimate personal occupational exposure that we are aware of. The sensor network achieved a high degree of spatial resolution, reducing errors related to spatial interpolation. We were able to estimate exposures at a relatively high temporal resolution, also an advantage over shift-long TWAs. We maintained a high degree of accuracy for the location information on simulated mobile employees with respect to both time and space with position diaries. Consequently, the location information we used to estimate personal exposures did not have errors that would have been inherent to those provided by in an indoor positioning system. Our multi-hazard sensor network was deployed at the study site continuously for nearly eight months. While we only had access to the facility for 5 days over that period to conduct personal sampling, we demonstrated the ability of our technique to potentially provide personal exposure estimates for any employee whose position can be tracked over that time. This kind of information on individual workers would be a vast improvement over traditional personal sampling rates [4, 5] with beneficial implications for both occupational exposure assessment for occupational exposure limit (OEL) compliance and epidemiological study.

Acknowledgements This project was funded through the National Institute for Occupational Safety and Health (NIOSH) under grant number R01 OH 010533. CZ was supported by the Johns Hopkins University Education and Research Center for Occupational Safety and Health (ERC), which is funded by NIOSH under grant number T42 OH 008428, and the University of Washington's Biostatistics, Epidemiology, and Bioinformatics Training in Environmental Heath (BEBTEH), grant number T32ES015459, from the National Institute for Environmental Health Science (NIEHS).

Compliance with ethical standards

Conflict of interest The authors declare that they have no conflict of interest.

References

1. Sferlazza SJ, Beckett WS. The respiratory health of Welders1-3. Am Rev Respir Dis. 1991;143:1134–48.
2. Rappaport SM, Kupper LL. Quantitative exposure assessment: S. Rappaport; 2008.
3. Rappaport SM. The rules of the game: an analysis of OSHA's enforcement strategy. Am J Ind Med. 1984;6:291–303.
4. Roick JC, Norwood SK, Hawkins NC. A strategy for occupational exposure assessment: AIHA; 1991.
5. Tornero-Velez R, Symanski E, Kromhout H, Yu RC, Rappaport SM. Compliance versus risk in assessing occupational exposures. Risk Anal. 1997;17:279–92.
6. Ramachandran G. Toward better exposure assessment strategies–the new NIOSH initiative. The Annals of Occupational Hygiene. 2008;52:297–301.
7. Rezagholi M, Mathiassen SE. Cost-efficient design of occupational exposure assessment strategies--a review. The Annals of Occupational Hygiene. 2010;54:858–68.
8. Kumar P, Morawska L, Martani C, Biskos G, Neophytou M, Di Sabatino S, et al. The rise of low-cost sensing for managing air pollution in cities. Environ Int. 2015;75:199–205.
9. Snyder EG, Watkins TH, Solomon PA, Thoma ED, Williams RW, Hagler GSW, et al. The changing paradigm of air pollution monitoring. Environ Sci Technol. 2013;47:11369.
10. Masson N, Piedrahita R, Hannigan M. Quantification method for electrolytic sensors in long-term monitoring of ambient air quality. Sensors. 2015;15:27283–302.
11. Piedrahita R, Xiang Y, Masson N, Ortega J, Collier A, Jiang Y, et al. The next generation of low-cost personal air quality sensors for quantitative exposure monitoring. Atmosph Measur Tech. 2014;7:3325.

12. Lewis AC, Lee JD, Edwards PM, Shaw MD, Evans MJ, Moller SJ, et al. Evaluating the performance of low cost chemical sensors for air pollution research. Faraday Discuss. 2016;189:85–103.
13. Jiang Q, Kresin F, Bregt AK, Kooistra L, Pareschi E, van Putten E, et al. Citizen sensing for improved urban environmental monitoring. J Sens. 2016;2016:5656245.
14. English PB, Olmedo L, Bejarano E, Lugo H, Murillo E, Seto E, et al. The imperial county community air monitoring network: a model for community-based environmental monitoring for public health action. Environ Health Perspect. 2017;125:074501.
15. Hasenfratz D, Saukh O, Walser C, Hueglin C, Fierz M, Arn T, et al. Deriving high-resolution urban air pollution maps using mobile sensor nodes. Pervasive Mobile Comput.2015;16:268–85.
16. Heimann I, Bright VB, McLeod MW, Mead MI, Popoola OAM, Stewart GB, et al. Source attribution of air pollution by spatial scale separation using high spatial density networks of low cost air quality sensors. Atmos Environ. 2015;113:10–9.
17. Kumar A, Singh IP, Sud SK. Energy efficient and low-cost indoor environment monitoring system based on the IEEE 1451 standard. IEEE Sensors J. 2011;11:2598–610.
18. Mead MI, Popoola OAM, Stewart GB, Landshoff P, Calleja M, Hayes M, et al. The use of electrochemical sensors for monitoring urban air quality in low-cost, high-density networks. Atmos Environ. 2013;70:186–203.
19. Ikram J, Tahir A, Kazmi H, Khan Z, Javed R, Masood U. View: implementing low cost air quality monitoring solution for urban areas. Environ Syst Res. 2012;1:1.
20. Moltchanov S, Levy I, Etzion Y, Lerner U, Broday DM, Fishbain B. On the feasibility of measuring urban air pollution by wireless distributed sensor networks. Sci Total Environ. 2015;502:537–47.
21. Jiao W, Hagler G, Williams R, Sharpe R, Brown R, Garver D, et al. Community Air Sensor Network (CAIRSENSE) project: evaluation of low-cost sensor performance in a suburban environment in the southeastern United States. Atmos Meas Tech. 2016;9:5281–92.
22. Gao M, Cao J, Seto E. A distributed network of low-cost continuous reading sensors to measure spatiotemporal variations of PM2. 5 in Xi'an, China. Environ Pollut. 2015;199:56–65.
23. Liu S, Hammond SK. Mapping particulate matter at the body weld department in an automobile assembly plant. J Occup Environ Hyg. 2010;7:593–604.
24. O'Brien DM. Aerosol mapping of a facility with multiple cases of hypersensitivity pneumonitis: demonstration of mist reduction and a possible dose/response relationship. Appl Occup Environ Hyg. 2003;18:947–52.
25. Heitbrink WA, Evans DE, Peters TM, Slavin TJ. Characterization and mapping of very fine particles in an engine machining and assembly facility. J Occup Environ Hyg. 2007;4:341–51.
26. Peters TM, Heitbrink WA, Evans DE, Slavin TJ, Maynard AD. The mapping of fine and ultrafine particle concentrations in an engine machining and assembly facility. Ann Occup Hyg. 2006;50:249–57.
27. Evans DE, Heitbrink WA, Slavin TJ, Peters TM. Ultrafine and respirable particles in an automotive grey iron foundry. Ann Occup Hyg. 2008;52:9–21.
28. Park JY, Ramachandran G, Raynor PC, Olson GM Jr. Determination of particle concentration rankings by spatial mapping of particle surface area, number, and mass concentrations in a restaurant and a die casting plant. J Occup Environ Hyg. 2010;7:466–76.
29. Vosburgh DJH, Boysen DA, Oleson JJ, Peters TM. Airborne nanoparticle concentrations in the manufacturing of polytetrafluoroethylene (PTFE) apparel. J Occup Environ Hyg. 2011;8:139–46.
30. Peters TM, Anthony TR, Taylor C, Altmaier R, Anderson K, O'Shaughnessy PT. Distribution of particle and gas concentrations in Swine gestation confined animal feeding operations. Ann Occup Hyg. 2012;56:1080–90.
31. Ott DK, Kumar N, Peters TM. Passive sampling to capture spatial variability in PM 10–2.5. Atmos Environ. 2008;42:746–56.
32. Koehler KA, Volckens J. Prospects and pitfalls of occupational hazard mapping: 'between these lines there be dragons'. Ann Occup Hyg. 2011;55:829–40.
33. Thomas G, Sousan S, Tatum M, Liu X, Zuidema C, Fitzpatrick M, et al. Low-cost, distributed environmental monitors for factory worker health. Sensors. 2018;18:1411.
34. Dockery DW. Epidemiologic study design for investigating respiratory health effects of complex air pollution mixtures. Environ Health Perspect. 1993;101(Suppl 4):187–91.
35. Anderson JO, Thundiyil JG, Stolbach A. Clearing the air: a review of the effects of particulate matter air pollution on human health. J Med Toxicol. 2012;8:166–75.
36. Pope CA, Dockery DW, Schwartz J. Review of epidemiological evidence of health effects of particulate air pollution. Inhal Toxicol. 1995;7:1–18.
37. Pope CA III, Dockery DW. Health effects of fine particulate air pollution: lines that connect. J Air Waste Manag Assoc. 2006;56:709–42.
38. Raub JA, Mathieu-Nolf M, Hampson NB, Thom SR. Carbon monoxide poisoning—a public health perspective. Toxicology. 2000;145:1–14.
39. Bornholdt J, Dybdahl M, Vogel U, Hansen M, Loft S, Wallin H. Inhalation of ozone induces DNA strand breaks and inflammation in mice. Mutation Res/Genet Toxico Environ Mutagen. 2002;520:63–72.
40. Lippmann M. Health effects of ozone a critical review. JAPCA. 1989;39:672–95.
41. Kampa M, Castanas E. Human health effects of air pollution. Environ Pollut. 2008;151:362–7.
42. Weschler CJ. Ozone's impact on public health: contributions from indoor exposures to ozone and products of ozone-initiated chemistry. Environ Health Perspect. 2006;114:1489–96.
43. Passchier-Vermeer W, Passchier WF. Noise exposure and public health. Environ Health Perspect. 2000;108(Suppl 1):123–31.
44. Zuidema C, Sousan S, Stebounova LV, Gray A, Liu X, Tatum M, et al. Mapping occupational hazards with a multi-sensor network in a heavy-vehicle manufacturing facility. Ann Work Exp Health. 2019;63:280–93.
45. Hallett L, Tatum M, Thomas G, Sousan S, Koehler K, Peters T. An inexpensive sensor for noise. J Occup Environ Hyg. 2018;15:448–54.
46. Berman JD, Peters TM, Koehler KA. Optimizing a sensor network with data from hazard mapping demonstrated in a heavy-vehicle manufacturing facility. Ann Work Expo Health. 2018;62:547–58.
47. Afshar-Mohajer N, Zuidema C, Sousan S, Hallett L, Tatum M, Rule AM, et al. Evaluation of low-cost electro-chemical sensors for environmental monitoring of ozone, nitrogen dioxide, and carbon monoxide. J Occup Environ Hyg. 2018;15:87–98.
48. Wang Y, Li J, Jing H, Zhang Q, Jiang J, Biswas P. Laboratory evaluation and calibration of three low-cost particle sensors for particulate matter measurement. Aerosol Sci Technol. 2015;49:1063–77.
49. Sousan S, Gray A, Zuidema C, Stebounova L, Thomas G, Koehler K, et al. Sensor selection to improve estimates of particulate matter concentration from a low-cost network. Sensors. 2018;18:3008.
50. Zuidema C, Afshar-Mohajer N, Tatum M, Thomas G, Peters T, Koehler K. Efficacy of paired electrochemical sensors for measuring ozone concentrations. J Occup Environ Hyg. 2018;16:179–90.
51. Sueur J, Aubin T, Simonis C. Seewave: a free modular tool for sound analysis and synthesis. Bioacoustics. 2008;18:213–26.

52. Bland JM, Altman D. Statistical methods for assessing agreement between two methods of clinical measurement. Lancet. 1986;327:307–10.
53. Sousan S, Koehler K, Thomas G, Park JH, Hillman M, Halterman A, et al. Inter-comparison of low-cost sensors for measuring the mass concentration of occupational aerosols. Aerosol Sci Technol. 2016;50:462–73.
54. Hossain M, Saffell J, Baron R. Differentiating NO_2 and O_3 at low cost air quality amperometric gas sensors. ACS Sensors. 2016;1:1291–4.
55. Spinelle L, Gerboles M, Aleixandre M. Performance evaluation of amperometric sensors for the monitoring of O_3 and NO_2 in ambient air at ppb level. Procedia Eng. 2015;120:480–3.
56. Beekhuizen J, Kromhout H, Huss A, Vermeulen R. Performance of GPS-devices for environmental exposure assessment. J Exp Sci Environ Epidemiol. 2013;23:498–505.
57. Adams C, Riggs P, Volckens J. Development of a method for personal, spatiotemporal exposure assessment. J Environ Monit. 2009;11:1331–9.
58. Mainetti L, Patrono L, Sergi I, editors. A survey on indoor positioning systems. 22nd International Conference on Software, Telecommunications and Computer Networks (SoftCOM); 2014.
59. Huang F-C, Shih T-S, Lee J-F, Chao H-P, Wang P-Y. Time location analysis for exposure assessment studies of indoor workers based on active RFID technology. J Environ Monit. 2010;12:514–23.
60. Khoury HM, Kamat VR. Evaluation of position tracking technologies for user localization in indoor construction environments. Autom Construct. 2009;18:444–57.
61. Sakata M, Yasumuro Y, Imura M, Manabe Y, Chihara K, editors. A Location Awareness System Using Wide-angle Camera and Active IR-Tag. MVA; 2002.
62. Bai YB, Wu S, Wu HR, Zhang K, editors. Overview of RFID-Based Indoor Positioning Technology. GSR; 2012: Citeseer.
63. Liu H, Darabi H, Banerjee P, Liu J. Survey of wireless indoor positioning techniques and systems. IEEE Trans Syst Man Cybernet Part C Appl Rev. 2007;37:1067–80.
64. Ahuja S, Potti P. An introduction to RFID technology. Commun Netw. 2010;2:183.
65. Lim MK, Bahr W, Leung SCH. RFID in the warehouse: a literature analysis (1995–2010) of its applications, benefits, challenges and future trends. Int J Prod Econ. 2013; 145:409–30.
66. Sharma D, Thomas GW, Foster ED, Iacovelli J, Lea KM, Streit JA, et al. The precision of human-generated hand-hygiene observations: a comparison of human observation with an automated monitoring system. Infect Control Hosp Epidemiol. 2012;33:1259–61.